Journal of Hard Tissue Biology 32[4] (2023) 213-222

CODEN-JHTBFF, ISSN 1341-7649

Original

Morphological Study for the Osteocytes in Podoplanin-Conditional Knockout Mice

Kyoko Osawa[1)], Takenori Kanai[1)], Natsumi Ushijima[2)], Koichiro Kajiwara[3)], Yoshihiko Sawa[4)] and Yoshiaki Sato[1)]

[1)] *Department of Orthodontics, Graduate School of Dental Medicine, Hokkaido University, Sapporo, Japan*
[2)] *Support Section for Education and Research, Graduate School of Dental Medicine, Hokkaido University, Sapporo, Japan*
[3)] *Department of Oral Growth & Development, Fukuoka Dental College, Fukuoka, Japan*
[4)] *Department of Oral Function & Anatomy, Graduate School of Medicine, Dentistry and Pharmaceutical Sciences, Okayama University, Okayama, Japan*
(Accepted for publication, September 29, 2023)

Abstract: We generated podoplanin-conditional knockout mice where the floxed podoplanin exon3 was deleted by the Dmp-1-driven Cre (*Dmp1-Cre;Pdpn$^{\Delta/\Delta}$*) and investigated the cell process elongation of podoplanin-deficient mouse osteocyte *in vitro* and *in vivo*. The expression of podoplanin is found in odontoblasts while not observed in odontoblasts of *Dmp1-Cre;Pdpn$^{\Delta/\Delta}$* mice, indicating that the conditional knockout of podoplanin in *Dmp1*-expressing cells in *Dmp1-Cre;Pdpn$^{\Delta/\Delta}$* mice is successful. There were no differences in the growth of wild-type and *Dmp1-Cre;Pdpn$^{\Delta/\Delta}$* mice, and no differences in calcification and alkaline phosphatase activity in cultured calvarial osteoblasts of the wild-type and *Dmp1-Cre;Pdpn$^{\Delta/\Delta}$* mice, in total this suggests that the podoplanin-cKO has no effect on generation of the bone. The cell process elongation was suppressed in cultured calvarial osteoblasts of *Dmp1-Cre;Pdpn$^{\Delta/\Delta}$* mice compared with wild-type mice. In the electron microscopic study, there were no morphological differences in bone matrix formation and osteocyte distribution in *Dmp1-Cre;Pdpn$^{\Delta/\Delta}$* and wild-type mice, whereas the cell process formation was sparser and the network with neighboring cells was more deficient in *Dmp1-Cre;Pdpn$^{\Delta/\Delta}$* mice than in wild-type mice. In the quantitative analysis, the number and thickness of the cell processes were significantly smaller and thinner in *Dmp1-Cre;Pdpn$^{\Delta/\Delta}$* mice than in wild-type mice. This could suggest that podoplanin plays a role in the formation of the osteocyte network created by the cell process elongation.

Key words: Podoplanin, cKO, Osteocyte

Introduction

Podoplanin is a mucin-like *O*-glycosylated transmembrane protein strongly negatively charged by sialic acid. Multiple terms corresponding to podoplanin have been reported by researchers for different areas like for the kidneys, lungs, bone, lymphatic vessels, and for cancer[1,2)]. The OTS-8 is the earliest report for podoplanin DNA[3)]. The OTS-8 is produced by the stimulation of the tumor promoter 12-O-tetradecanoylphorbol-13-acetate as the early response protein in the mouse osteoblast-like MC3T3-E1 cells. The gp38 is reported as the 38 amino acid sequence of the mouse thymic epithelial epitope recognized by a hamster anti-podoplanin monoclonal antibody produced from the clone 8.1.1[4)]. The gp38 closely resembles OTS-8 and human podoplanin gp36. The E11 is a podoplanin antigen recognized by a monoclonal antibody to the rat osteoblastic osteosarcoma cell line ROS17/2.8[5-7)]. The E11 has been extensively researched as a mature late osteoblast and osteocyte marker in dendrites other than dentin matrix protein 1 (DMP-1) and sclerostin in mature osteoblast/osteocytes and expression increases in the MC3T3-E1 and human osteoblast-like MG63 cells in calcification medium. The MLO-Y4 and IDG-SW3 are the osteocyte-like cells which the expression amounts of podoplanin are more strongly than MC3T3-E1 in the mouse long bone[8-15)].

Correspondence to: Dr. Yoshihiko Sawa, Department of Oral Function & Anatomy, Okayama University Graduate School of Medicine, Dentistry and Pharmaceutical Sciences, 2-5-1 Shikata-cho, Okayama Kita-ku, 700-0914 Japan; Tel: +81-86-235-6635; Fax: +81-86-235-6639; E-mail: ysawa@okayama-u.ac.jp.

Podoplanin is a ligand to the platelet transmembrane protein C-type lectin-like receptor CLEC-2 and is able to bind platelets by the functional residues including *O*-glycosylated Thr52[16-18)]. Podoplanin binds CLEC-2 and induces the association of podoplanin cytoplasmic parts with CD44 on podoplanin-positive cells via the assembly of ezrin-radixin-moesin (ERM)[19-20)]. The cell shape and cytoskeleton arrangement are controlled by the ERM-actomyosin assembly formation via podoplanin expression on the cell membrane and binding of podoplanin with CLEC-2 induces the separation of the ERM-actomyosin assembly. For example, in lymph nodes fibroblastic reticular cells contract cell processes dependent on the property of podoplanin which induces ERM phosphorylation. The phospho-ERM induces the rearrangement of actomyosin and elongates cell process in fibroblastic reticular cells. The lymph node expansion causes by the reduction of podoplanin-mediated contraction in inflamed lymph nodes where mature dendritic cells interact with fibroblastic reticular cells via podoplanin-CLEC-2 binding[21-24)]. There is a detailed report on the expression of podoplanin in bone cells[25)]. It shows that the CD44-podoplanin binding contributes to the osteoblast differentiation in the remodeling sites but not in modeling sites of bone. Taken together, podoplanin may function in the osteocyte cell shape formation via osteoblastic differentiation. This study aims to investigate the cell process formation of osteocytes in the bones of podoplanin-cKO mice by an electron microscopic study.

Materials and Methods

The goal of animal use in the present study was to clarify the forma-

tion of osteocyte cell processes in mice where podoplanin alleles are inactivated in osteocytes and odontoblasts. The manuscript was prepared following the ARRIVE guidelines. All procedures of animal care and use were performed according to the applicable international, national and institutional guidelines and regulations. We obeyed ethical standards of the institutional and national research committees, and 1964 Helsinki declaration, and its later amendments or comparable ethical standards described elsewhere[26,27]. The animal experimental protocol was approved by the Animal Experiment Committee of Fukuoka Dental College (No. 17018). All animal maintanance and experiments were conducted in the Fukuoka Dental College Animal Center following the conditions and procedures described elsewhere[28,29]. The health check was daily assessed by humane endpoints. Mice with humane endpoints of lost ability to ambulate (inability to access food or water) were promptly euthanized by induction anesthesia with intraperitoneal injections of sodium pentobarbital and cervical dislocation. All data of mice employed were involved in the experimental and control data without exclusions.

Animals

The procedures are described elsewhere[26,27]. For breeding, the studies here used 4-week-old three type mice (2 pairs in each): C57BL/6N wild-type mice with normal podoplanin alleles purchased from a commercial vendor (Kyudo, Fukuoka, Japan), C57BL/6.FVB-Tg (*Dmp1*-Cre) 1Jqfe/BwdJ (*Dmp1*-Cre) purchased from a commercial vendor (Jax Strain #023047), and C57BL/6N with floxed *Pdpn* exon3 alleles ($Pdpn^{fl/fl}$). We finally acquired $Pdpn^{fl/fl}$ x *Dmp1-Cre* mice with $Pdpn^{\Delta/\Delta}$ alleles in *Dmp1* expressing cells ($Pdpn^{\Delta/\Delta}$) and used mice with three type podoplanin alleles (wild-type, $Pdpn^{fl/fl}$, $Pdpn^{\Delta/\Delta}$). The animal maintenance and experiments were healthily performed with normal feeding under a conventional 100% controlled atmosphere passed an examination for bacteria in a room of the Fukuoka Dental College Animal Center. Mice were maintained in two/cage with an inverse 12-hr day-night cycle with lights on from 7:00 p.m. The temperature was controlled at 22°C with a-55% humidity. All specimens were collected from mice euthanized. The induction of anesthesia was performed by the 2% isoflurane (1 l/min) mixed with 30% oxygen and 70% nitrous oxide followed by cervical dislocation and intraperitoneal injections with sodium pentobarbital (150 mg/kg; Sumitomo Dainippon Pharma Co., Ltd., Tokyo, Japan) at the end of the designated period of the experiments. In summary, 6 mice in each group of the wild-type, $Pdpn^{fl/fl}$ and *Dmp1-Cre;*$Pdpn^{\Delta/\Delta}$ mice were used to investigate the characteristics of cultured odontoblasts isolated from one-week-old mouse calvaria for the *in vitro* study and of osteocytes in 23-week mouse femur for the microscopic study.

Generation of knockout mice

The method to generate mice carrying the homozygous floxed podoplanin allele ($Pdpn^{fl/fl}$) is described elsewhere[27]. Briefly, the $Pdpn^{tm1a(EUCOMM)Wtsi}$ having the genetic background of C57BL/6N-A^{tm1Brd} was used with the *Pdpn* targeting vector HTGR03003_Z_2_G05 (EUCOMM) to generate knockout first. The targeted allele with the gene trap cassette ($Pdpn^{gt}$) is used as a conventional knockout-first allele to disrupt the targeted *Pdpn* splicing in C57BL/6N embryonic stem (ES) cells. The construct was knocked into the Pdpn locus (GeneID: 14726, chromosome 4) by homologous recombination. The Pdpn gene sandwiched by loxP is ENSMUSE00000180432 in the Ensemble database, and exon3 in NM_010329 in the NCBI database. The generation of *Pdpn* gene knockout-first allele ($Pdpn^{KO1st}$) were achieved from chimeric mice with the *Pdpn*-targeted ES cells in which the genetic background is C57BL/6NCrj. The promoter-driven targeting cassette is flanked by flippase (Flp) recognition target FRT sites and the removal of the targeting cassette by Flp generates a *Pdpn* conditional knockout (cKO) allele including loxP sites flanking exon 3 ($Pdpn^{fl}$, floxed exon 3). All transcript variants of *Pdpn* have exon3 and the deletion of exon 3 causes a frameshift mutation leading to premature stop codon. The exon 3 deletion stops prematurely by forming a stop codon near the 5′ end of exon 4 or 5 depending on splicing variants, thereby disrupting translation of the *Pdpn* ($Pdpn^{\Delta}$). Mice expressing $Pdpn^{gt}$ allele heterozygously were mated with mice having Flp, *ACTB:FLPe* (B6;SJL-Tg(ACTFLPe)9205Dym/J, JAX 003800) to leave $Pdpn^{fl}$. In this study, C57BL/6.FVB-Tg (*Dmp1*-cre) 1Jqfe/BwdJ, carrying alleles with dentin matrix acidic phosphoprotein 1 (*Dmp1*) promotor-driving *Cre* recombinase gene expressing tissue-specific heterozygously, was used to delete $Pdpn^{fl}$. The mice simultaneously having homozygous $Pdpn^{fl}$ alleles ($Pdpn^{fl/fl}$) and heterozygous allele were used as a true conditional knockout for podoplanin in *Dmp1*-expressing osteocytes and odontoblasts (*Dmp1-Cre*;$Pdpn^{\Delta}$).

Cell culture

Primary osteoblasts of neonate calvaria were collected following a protocol previously used[28-30]. In brief, neonatal mice were euthanized by anesthesia and cervical dislocation, and treated by collagenase with 0.25% trypsin with 5 sequential 30-min digestions at 37°C. Cell frac-

Table 1. Sequence of primers

Genotyping				
RefSeq	DNA	forward (5'-3')	Tm (°C)	bp
		reverse (5'-3')		
MGI 4842558	gPdpn1	AGGAAGAATCCCACACCAGG	57.6	128/208
		TGTAGGGAGCTACCGCTAGG	58.9	
	gPdpn2	GAAGTTCCTATTCCGAAGTTCC	59.3	174/1096
		CCGCTAGGTATCATTCAAGGTTAAGA	58.7	
	gPdpn3	TCTTCTCTCTTTCTTTCCTCACTTCT	59.3	207
		TCCCGCCTCTTGGACCCA	58.7	
KC845567.1	Cre	CGTTTTCTGAGCATACCTGGA	60.1	472
		ATTCTCCCACCGTCAGTACG	60.1	

Gene symbols are described according to international notation.

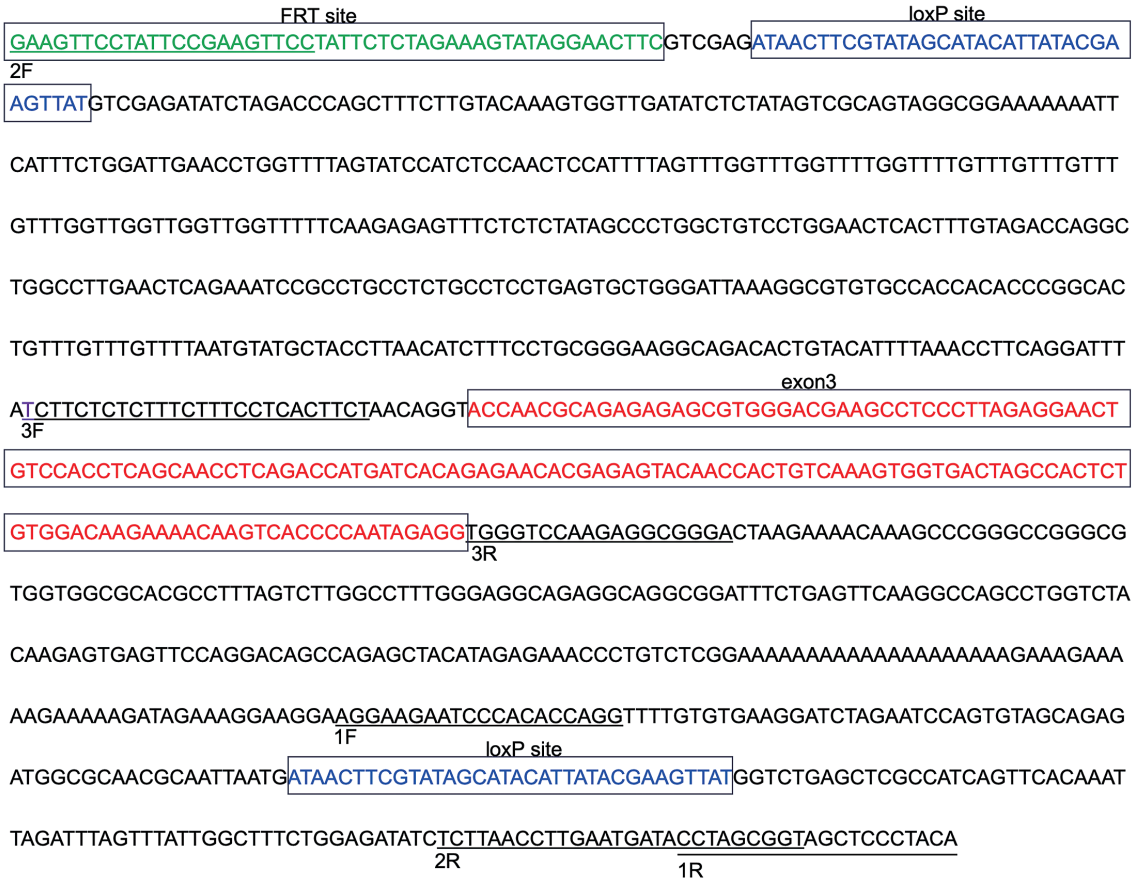

Figure 1. Gene map for genotyping. The gPdpn1 primers were designed flanking the loxP after the *Pdpn* exon 3 in the allele of $Pdpn^{fl}$ (208 bp) and the PCR products for the podoplanin wild-type allele show 128 bp. The gPdpn2 primers were designed flanking the FRT site and loxP after the *Pdpn* exon 3 (1,096 bp), and the PCR products for the $Pdpn^{\Delta}$ allele show 174 bp. The gPdpn3 primers were designed flanking the *Pdpn* exon 3 (207 bp).

Table 2. Sequence of primers

RT-PCR				
RefSeq	mRNA	forward (5'-3')	Tm (°C)	bp
		reverse (5'-3')		
NM_007393	Actb	GTTCTACAAATGTGGCTGAGGA	60.1	411
		ATTGGTCTCAAGTCAGTGTACAG	58.8	
NM_010329	Pdpn	CACCTCAGCAACCTCAGAC	54.5	192
		ACAGGGCAAGTTGGAAGC	54.2	
NM_016779	DMP1	TGTGCTCTCCCAGTTGCCAG	59.3	165
		ACTGCTGTCCGTGTGGTCA	58.1	

Gene symbols are described according to international notation.

tions from the third to fifth digestion were collected and seeded on collagen-coated 24-well culture plates (Asahi Glass Co., LTD., Shizuoka, Japan). The primary cells were cultured in Minimum Essential Medium Eagle, Alpha Modification (α-MEM, Sigma-Aldrich Corp. LLC., St. Louis, MO, USA) with 10% fetal bovine serum (Biowest, Nuaillé, France) for 10 days and harvested, and then cultured in calcification medium of a mouse osteogenesis culture medium kit (Cosmo Bio, Tokyo, Japan) containing 100 nM dexamethasone, 50 μg/ml, ascorbic acid, and 10 mM β-glycerophosphate in collagen-coated 6-well culture plates for 20 days. The culture was fixed by 10% formalin-phosphate-buffered saline (PBS) and stained by 40 mM alizarin red S (pH 4.2) using a Calcified Nodule Staining kit (Cosmo Bio) for 30 min at room temperature. The culture was washed 3 times with distilled water and was added by 5% formic acid to dissolve the alizarin red-stained calcified nodules. The establishment of osteoblasts was determined by the detection of alizarin red staining and alkaline phosphatase activity (Cosmo Bio), and by the detection of podoplanin and Dmp1 mRNAs.

Genotyping and reverse transcription polymerase chain reaction (RT-PCR)

The method is described elsewhere[27]. Briefly, genomic DNA from the tail was isolated with a QIAamp DNA Blood and Tissue Kit (Qiagen, Inc., Hilden, Germany). The RT-PCR was also performed to detect the podoplanin mRNA in the cultured osteoblasts from calvaria. All procedures were performed according to protocols provided by the manufacturers. Total RNA extraction from the primary cell culture in a mouse osteogenesis culture medium kit (Cosmo Bio) was performed with a QIAshredder column and RNeasy kit (Qiagen, Inc., Tokyo, Japan) and the RT was performed on 30 ng of total RNA. The PCR was performed for the gemonic DNA and RT products by 30 cycles of amplification using the Ex Taq hot start version (Takara Bio Inc., Shiga, Japan). This study used the primer sets (50 pM) which had been confirmed the specificities by the manufacturer (Table 1; Sigma-Aldrich Corp., Tokyo, Japan). The PCR products were separated on 2% agarose gel (NuSieve 3:1 Agarose; FMC Bio Products, Rockland, ME, USA) and visualized by Syber Green (Takara Bio Inc.). The correct size of the amplified PCR products was confirmed by gel electrophoresis and the amplification of accurate targets was confirmed by sequence analysis. For genotyping (Table 1, Fig.1), the gPdpn1 primer set was designed flanking loxP after exon 3 in the allele of *Pdpn*^{fl} (208 bp) and the wild-type *Pdpn* gene without loxP shows 128 bp. The gPdpn2 primer set was designed flanking exon 3 and loxP (1,096 bp), and the *Pdpn*$^{\Delta}$ allele deleted this region

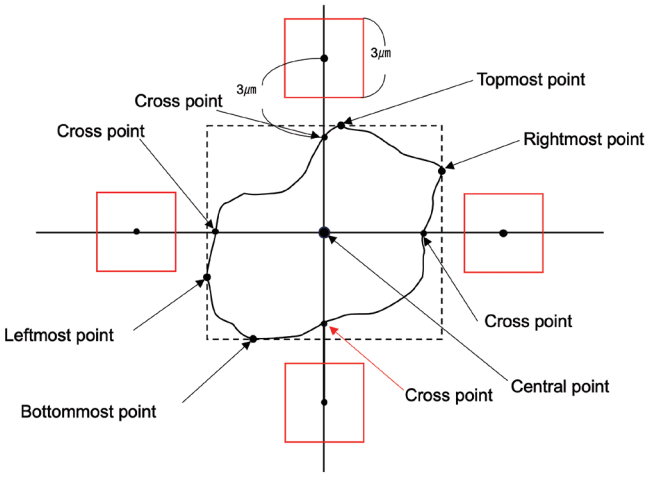

Figure 2. Measuring the range of osteocyte dendrites. A rectangle (dotted line) was constructed by four tangential lines to the four points of osteocyte margin (Topmost, Bottommost, Leftmost, Rightmost) and the center of the rectangle (Central point) was determined as the center of the osteocyte. The horizontal and intersecting axes passing through Central point were constructed and the four intersections with the margin of the osteocyte (Cross point) were determined. The number and thickness of osteocytes were measured in four 3.0-μm squares (red) where the center of the square is 3.0 μm away from Cross point.

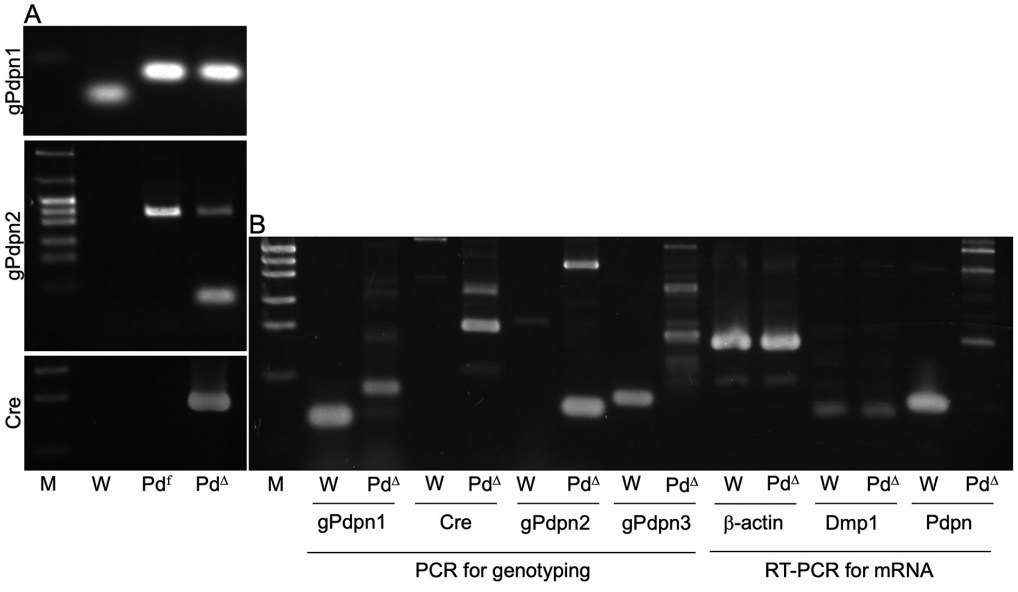

Figure 3. Genotyping and RT-PCR of tail and cultured osteoblasts. (A) The genotyping of the tail. For the gPdpn1, the gene containing loxP after the *Pdpn* exon 3 in the allele of the *Pdpn*^{fl} (208 bp) was detected from the tails of the *Pdpn*$^{fl/fl}$ mice and *Dmp1-Cre;Pdpn*$^{\Delta/\Delta}$ mice, while the gene without loxP after *Pdpn* exon 3 was detected from the wild-type mice (128 bp). For the gPdpn2, the gene flanking the FRT and loxP after the *Pdpn* exon 3 (1,096 bp) in the allele of *Pdpn*^{fl} was detected from the tail of the *Pdpn*$^{fl/fl}$ mice while not detected from the tail of the wild-type mice. Both of the intact gene (1,096 bp) and the gene cleaved by the Cre recombinase (174 bp) was detected from the *Dmp1-Cre;Pdpn*$^{\Delta/\Delta}$ mice. The gene of Cre recombinase (472 bp) was detected from the tail of the *Dmp1-Cre;Pdpn*$^{\Delta/\Delta}$ mice. (B) The genotyping and RT-PCR of cultured osteoblasts. For the gPdpn1, the gene containing loxP after the *Pdpn* exon 3 (208 bp) was detected from the cultured osteoblasts of *Dmp1-Cre;Pdpn*$^{\Delta/\Delta}$ mice while the gene without loxP after the *Pdpn* exon 3 was detected from the wild-type mice (128 bp). The gene of Cre recombinase (472 bp) was detected from the cultured osteoblasts of *Dmp1-Cre;Pdpn*$^{\Delta/\Delta}$ mice while not detected from the cultured osteoblasts of the wild-type mice. For the gPdpn2, both of the gene flanking the FRT and loxP after the *Pdpn* exon 3 (1,096 bp) and the gene cleaved by the Cre recombinase (174 bp) were detected from the cultured osteoblasts of *Dmp1-Cre;Pdpn*$^{\Delta/\Delta}$ mice, while not detected from cultured osteoblasts of wild-type mice. For the gPdpn3, the gene flanking the *Pdpn* exon 3 (207 bp) was detected from the cultured osteoblasts of the wild-type mice while not detected from the cultured osteoblasts of the *Dmp1-Cre;Pdpn*$^{\Delta/\Delta}$ mice. For RT-PCR, the mRNAs of β-actin (411 bp) and DMP-1 (165 bp) were detected at the same level from the cultured osteoblasts of both the wild-type and *Dmp1-Cre;Pdpn*$^{\Delta/\Delta}$ mice. The mRNAs of podoplanin (Pdpn, 192 bp) were detected from the cultured osteoblasts of wild-type mice but not from the cultured osteoblasts of *Dmp1-Cre;Pdpn*$^{\Delta/\Delta}$ mice. M: molecular weight marker; W: wild-type, Pd^{f}: *Pdpn*$^{fl/fl}$; Pd$^{\Delta}$: *Pdpn*$^{\Delta/\Delta}$

resulted in 174 bp. The gPdpn3 primer set was designed flanking *Pdpn* exon 3 in the allele of *Pdpn*^{fl} (207 bp). The primer set for the Cre recombinase which is driven by *Dmp1* promoter was designed to detect a part of the Cre gene (472 bp). For RT-PCR (Table 2, Fig.1), primer sets were also designed for common regions in all splicing variants of podoplanin (192 bp) and Dmp1 (165 bp) mRNAs.

Immunohistochemistry

The method is described elsewhere[26,27]. Briefly, frozen 10 μm-sections were cut and fixed in 100% methanol for 30 sec at -20°C, treated with 0.1% goat serum for 30 min at 20°C, and then treated for 8 hrs at 4°C with PBS containing 0.1% goat serum and 1 μg/ml hamster monoclonal anti-mouse podoplanin (BioLegend, Inc., San Diego, CA, USA). The sections were washed three times in PBS for 10 min and treated for 0.5 hr at 20˚C with 0.1 μg/ml of Alexa Fluor 568-conjugated goat anti-hamster IgG (Thermo Fisher Scientific Inc., Waltham, MA, USA). The immunostained sections were mounted in 50% polyvinylpyrrolidone solution and examined by fluorescence microscopy (BZ-8100, Keyence Corp., Osaka, Japan) or confocal laser-scanning microscopy (LSM710, Carl Zeiss, Jena, Germany) with an x63 oil Plan Apochromatic objective lens.

Transmission electron microscopic study

The femur specimens of wild-type and *Pdpn*$^{\Delta/\Delta}$ mice were fixed with 4% paraformaldehyde-PBS. After washing, specimens were immersed in a decalcifying solution (G-Chelate/Quick, GenoStaff Inc., Tokyo, Japan; 4°C, for 7 days) and in the neutralization solution (G-Chelate/NT, GenoStaff; 4°C, 12 hr). After the treatment in 30% potassium hydroxide

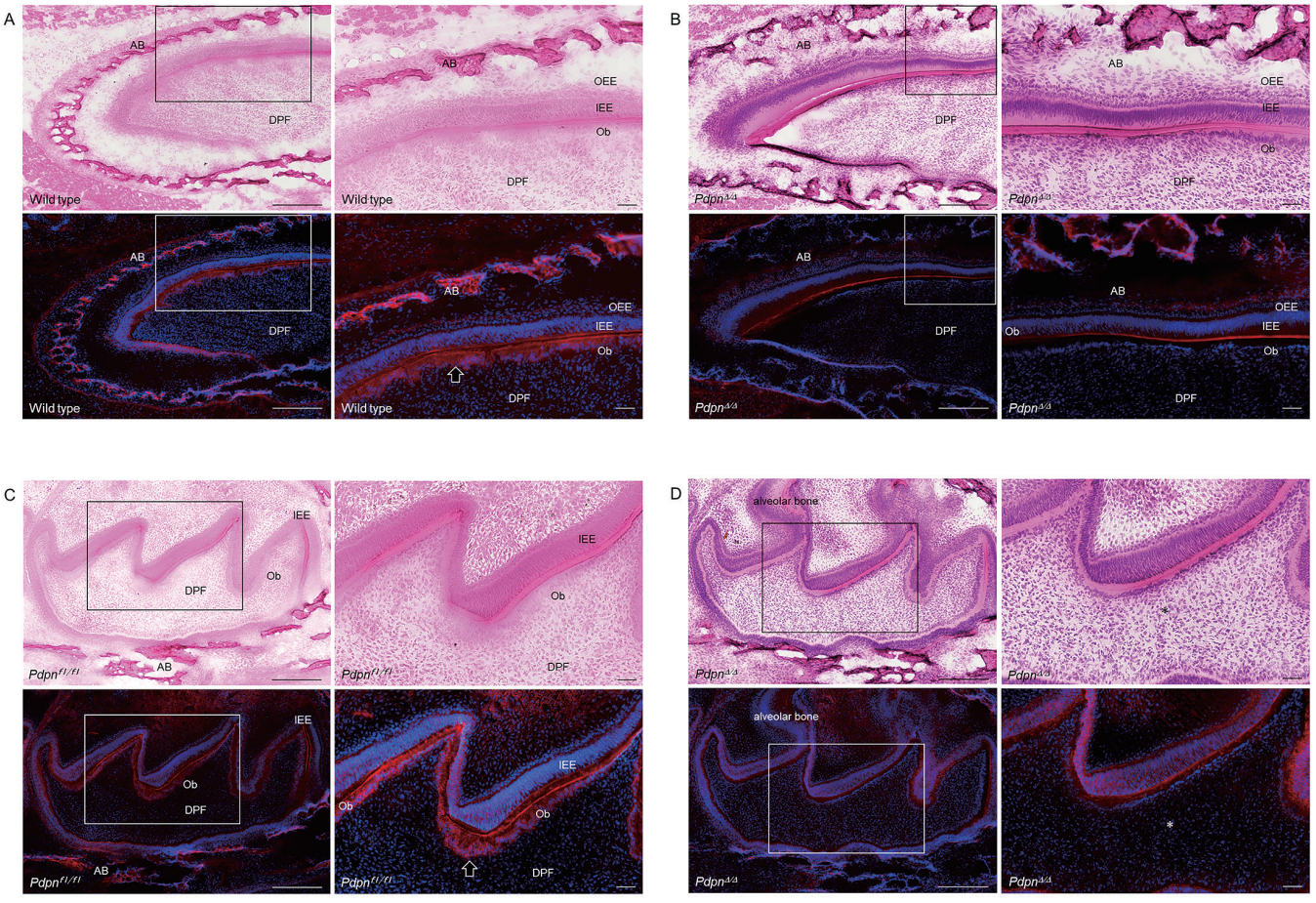

Figure 4. Immunostaining of podoplanin in the one-week mouse odontoblasts. (A) Immunostaining of podoplanin in the one-week wild-type mouse lower incisor sagittal section. In the right images at the higher magnification of the parts highlighted by the boxes in the left panels, the expression of podoplanin (arrow) is observed in the odontoblasts (Ob), in the inner enamel epithelial cells (IEE), and in the outer enamel epithelial cells (OEE), but not in the dental pulp fibroblasts (DPF). The podoplanin expression is also observed in the alveolar bone. Bar: 100 μm. (B). Immunostaining of podoplanin in the one-week *Dmp1-Cre;Pdpn*$^{\Delta/\Delta}$ mouse lower incisor sagittal section. In the right images at the higher magnification of the parts highlighted by the boxes in the left panels, the expression of podoplanin is not observed in the odontoblasts (Ob) as well as not in the dental pulp fibroblasts (DPF), while the expression is observed in the inner enamel epithelial cells (IEE) and in the outer enamel epithelial cells (OEE). The cross-reaction to the bone is also observed. Bar: 100 μm. (C) Immunostaining of podoplanin in the one-week *Pdpn*$^{fl/fl}$ mouse molar sagittal section. In the right images at the higher magnification of the parts highlighted by the boxes in the left panels, the expression of podoplanin is observed in the odontoblasts (Ob), in the inner enamel epithelial cells (IEE), and in the outer enamel epithelial cells (OEE), but not in the dental pulp fibroblasts (DPF). Bar: 100 μm. (D) Immunostaining of podoplanin in the one-week *Dmp1-Cre;Pdpn*$^{\Delta/\Delta}$ mouse molar sagittal section. In the right images at the higher magnification of the parts highlighted by the boxes in the left panels, the expression of podoplanin is not observed in the odontoblasts (Ob) as well as in the dental pulp fibroblasts (DPF), while the expression is observed in the inner enamel epithelial cells (IEE) and in the outer enamel epithelial cells (OEE). Bar: 100 μm.

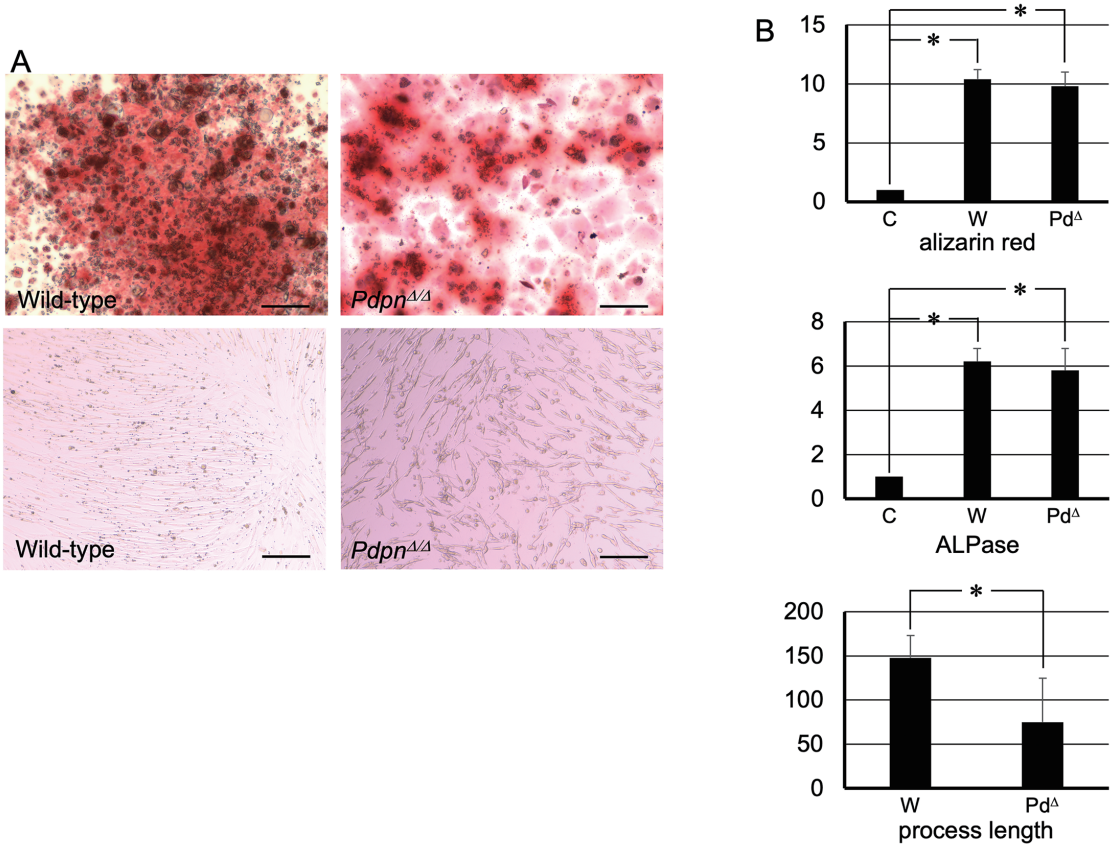

Figure 5. Calcification, alkaline phosphatase activity and length of cultured mouse osteoblasts. (A) Microscopic observations of cultured calvarial osteoblasts. Alizarin red staining of cells cultured in calcification medium is shown in top panels. Calcification is observed in cells established from *Dmp1-Cre;Pdpn*$^{\Delta/\Delta}$ mice (*Pdpn*$^{\Delta/\Delta}$) as well as in cells established from wild-type mice (Wild-type). The shape of cells cultured in α-MEM is shown in bottom panels. Normal cell elongation is observed in culture of Wild-type while small and round cells were observed in of *Pdpn*$^{\Delta/\Delta}$. (B) Quantitative analysis of cultured calvarial osteoblasts for calcified nodule amounts (top graph), alkaline phosphatase activities (middle graph) and cell lengths (bottom graph). The alizarin red-stained calcified nodules were dissolved by formic acid and the absorbances were measured at 450 nm. Relative calcification amounts were expressed in arbitrary units, calculated according to the following formula: solution of calcified nodules of culture with calcification medium / the solution of culture with α-MEM. Calcified nodule amounts of the culture of wild-type mice with calcification medium (W) and the culture of *Dmp1-Cre;Pdpn*$^{\Delta/\Delta}$ mice with calcification medium (Pd$^{\Delta}$) are larger than the control culture of wild-type mice with α-MEM (C). Calcified nodule amounts in Pd$^{\Delta}$ are not significantly different from W. Alkaline phosphatase activities were determined by the absorbance of catalyzed pNPP at 405 nm. Relative alkaline phosphatase activities were expressed in arbitrary units, calculated according to the following formula: activities of culture with calcification medium / activity of control culture with α-MEM. Alkaline phosphatase activities of the culture of wild-type mice with calcification medium (W) and the culture of *Dmp1-Cre;Pdpn*$^{\Delta/\Delta}$ mice with calcification medium (Pd$^{\Delta}$) are larger than the control culture of wild-type mice with α-MEM (C). The alkaline phosphatase activity of Pd$^{\Delta}$ is not significantly different from W. The cell length average was significantly shorter in *Dmp1-Cre;Pdpn*$^{\Delta/\Delta}$ (Pd$^{\Delta}$) than in wild-type mice (W). *Significantly different (p<0.001).

(60°C, 7 min) specimens were dehydrated in 70, 80, 90 and 100% ethanol at RT for 30 min each. The specimens were treated with critical point drying by Hitachi HCP-1 at 37°C in 80 atm for 1 hr and adhered to the sample stage with carbon double-sided tape. The specimens were treated with platinum palladium coating by Hitachi E-1030 for 120 s and observed by SEM (Hitachi S4800; Electron gun acceleration voltage: 5.0 kV, magnification: ×5.00 k). The osteocyte dendritic network was measured on five different spots (0.36 mm x 0.36 mm) in the renal section images using ImageJ (National Institutes of Health, Bethesda, MD) (Fig. 2). The edge of the osteocyte of photograph was traced on graph paper and the center of the osteocyte obtained as determined from the highest point, the lowest point, the leftmost point, and the rightmost point of the osteocyte. Four points at which the edge of the osteocyte intersects with each of the vertical and horizontal axes drawn from the central point were determined. Four squares with sides of 3.0 μm were drawn centering on a point 3.0 μm away on the axis from each of the four points and the numbers of cell processes in the squares were counted, followed by the calculation of the mean number of cell processes per 1.0μm^2.

Statistics

All experiments were carried out 10 times, repeatedly, and data are expressed as mean + SD. The determination of statistically significant differences (p< 0.01) was assessed by one-way ANOVA and the unpaired two-tailed Student's t-test with STATVIEW 4.51 software (Abacus concepts, Calabasas, CA, USA).

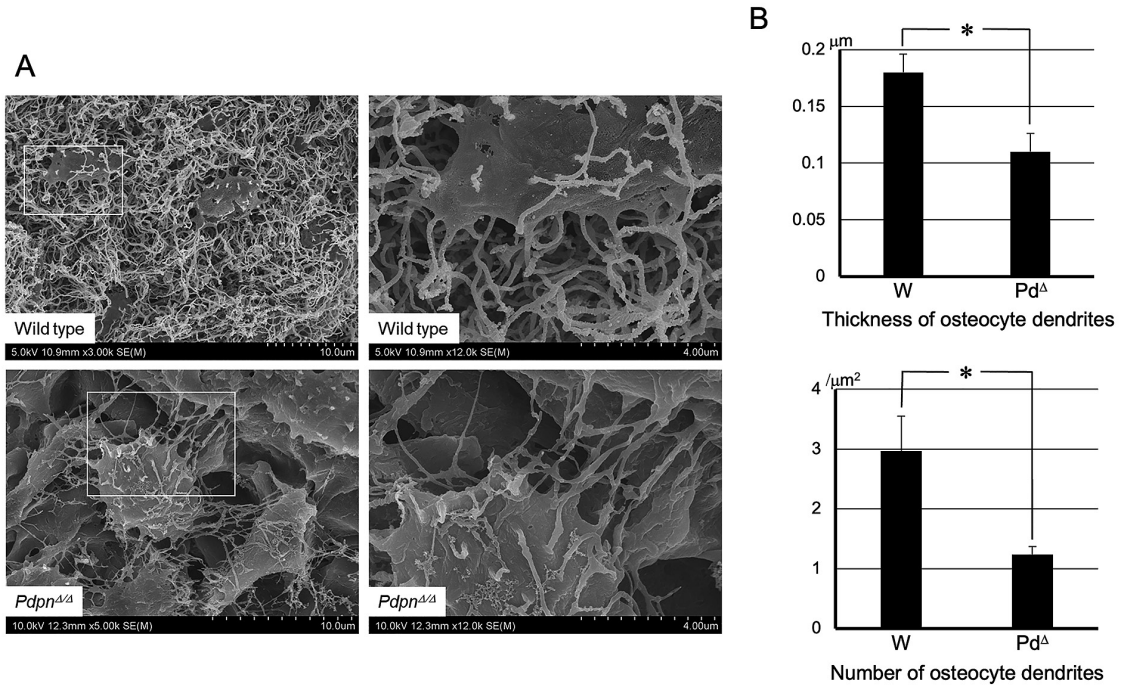

Figure 6. TEM analysis for osteocytes in *Dmp1-Cre;Pdpn*$^{\Delta/\Delta}$ mouse femur. (A) Microscopic observations. In the right images at the higher magnification of the parts highlighted by the boxes in the left panels. Well-developed osteocyte processes are observed in the wild-type mouse femurs. There were no significant differences in bone matrix formation and osteocyte distribution in the *Dmp1-Cre;Pdpn*$^{\Delta/\Delta}$ compared to the wild-type mice. However, the process formation and the network with neighboring cells are less well developed in *Dmp1-Cre;Pdpn*$^{\Delta/\Delta}$ than in wild-type mice. (B) Quantitative analysis. The number and thickness of cell processes are significantly smaller and thinner in *Dmp1-Cre;Pdpn*$^{\Delta/\Delta}$ mice (Pd$^{\Delta}$) than in wild-type and *Pdpn*$^{fl/fl}$ mice (W). *Significantly different (p<0.001).

Results

Genotyping of Pdpn exon3, Cre, and FRT genes in Dmp1-Cre;Pdpn$^{\Delta/\Delta}$ *mouse tail and cultured osteoblasts isolated from calvaria*

For the genotyping of the tail, the gene containing loxP after *Pdpn* exon 3 in the allele of *Pdpn*^{fl} was detected in *Pdpn*$^{fl/fl}$ mice and *Dmp1-Cre;Pdpn*$^{\Delta/\Delta}$ mice, while the gene without loxP after the *Pdpn* exon 3 was detected in wild-type mice (Fig. 3). The gene flanking FRT and loxP after *Pdpn* exon 3 in the allele of *Pdpn*^{fl} was detected in the *Pdpn*$^{fl/fl}$ mice while not detected in wild-type mice. Both the intact gene and the cleaved podoplanin gene were detected in *Dmp1-Cre;Pdpn*$^{\Delta/\Delta}$ mice. The gene of Cre recombinase was detected in *Dmp1-Cre;Pdpn*$^{\Delta/\Delta}$ mice. For genotyping of cultured calvarial osteoblasts, the gene containing loxP after *Pdpn* exon 3 in the allele of *Pdpn*^{fl} was detected in *Dmp1-Cre;Pdpn*$^{\Delta/\Delta}$ mice while genes without loxP after *Pdpn* exon 3 was detected in wild-type mice (Fig. 3). The gene of Cre recombinase was detected in *Dmp1-Cre;Pdpn*$^{\Delta/\Delta}$ mice. Both of the genes flanking FRT and loxP after *Pdpn* exon 3, and the cleaved podoplanin gene were detected in *Dmp1-Cre;Pdpn*$^{\Delta/\Delta}$ mice, while it was not detected in wild-type mice. The gene flanking *Pdpn* exon 3 was detected in wild-type mice while it was not detected in *Dmp1-Cre;Pdpn*$^{\Delta/\Delta}$ mice. For RT-PCR of cultured osteoblasts, the mRNAs of β-actin and DMP-1 were detected in both wild-type mice and *Dmp1-Cre;Pdpn*$^{\Delta/\Delta}$ mice in similar intensities (Fig. 3). The mRNAs of *Pdpn* were detected in wild-type mice but not in *Dmp1-Cre;Pdpn*$^{\Delta/\Delta}$ mice.

Immunostaining of Dmp1-Cre;Pdpn$^{\Delta/\Delta}$ *mouse teeth for podoplanin*

In the one-week-old wild-type and *Pdpn*$^{fl/fl}$ mouse tissue, the expression of podoplanin was observed in the odontoblasts, inner and outer enamel epithelial cells and pre-ameloblasts in the incisors and molars (Fig. 4). The expression of podoplanin was also observed in the alveolar bone while it was not observed in the dentin, dental pulp fibroblasts, pre-odontoblasts, periodontal ligament, or bone marrow. In the one-week-old *Dmp1-Cre;Pdpn*$^{\Delta/\Delta}$ mouse tissue, the expression of podoplanin was observed in the inner and outer enamel epithelial cells and pre-ameloblasts but not in the odontoblasts in the incisors and molars, which were PDPN-positive in wild-type and *Pdpn*$^{fl/fl}$ mice (Fig. 4). There were no abnormalities in the tooth or bone development in the *Dmp1-Cre;Pdpn*$^{\Delta/\Delta}$ mouse tissue.

Calcification, alkaline phosphatase activity and cell process elongation of cultured mouse osteoblasts

In calcification medium cultured calvarial osteoblasts isolated from *Dmp1-Cre;Pdpn*$^{\Delta/\Delta}$ mice showed calcified nodules stained by alizarin red and alkaline phosphatase activity (Fig. 5). There were no differences in the calcification and alkaline phosphatase activity in cultured calvarial osteoblasts of wild-type mice and *Dmp1-Cre;Pdpn*$^{\Delta/\Delta}$ mice. Cell process elongation was observed in cultured calvarial osteoblasts of wild-type mice while the elongation was suppressed in cultured calvarial osteoblasts of *Dmp1-Cre;Pdpn*$^{\Delta/\Delta}$ mice.

Morphological analysis for osteocytes in Dmp1-Cre;Pdpn$^{\Delta/\Delta}$ *mouse femur*

Highly-developed networks of osteocyte processes were observed in the femur of both wild-type and *Dmp1-Cre;Pdpn*$^{\Delta/\Delta}$ mice (Fig. 6). The process formation was sparser and the network formation with neighboring cells was more deficient in *Dmp1-Cre;Pdpn*$^{\Delta/\Delta}$ mice than in wild-

type mice. There were no morphological differences in bone matrix formation and osteocyte distribution in *Dmp1-Cre;Pdpn*$^{\Delta/\Delta}$ compared with wild-type mice. In the quantitative analysis, the number and thickness of cell processes were significantly lesser and thinner in *Dmp1-Cre;Pdpn*$^{\Delta/\Delta}$ mice than in wild-type mice. There were no differences in the body growth between *Dmp1-Cre;Pdpn*$^{\Delta/\Delta}$ mice and wild-type.

Discussion

Generation of Dmp1-Cre;Pdpn$^{\Delta/\Delta}$ *mice*

Previously we first reported that podoplanin-cKO mice in which Cre recombinase driven by the wingless-related MMTV integration site one promoter targets the gene of podoplanin exon 3 in cranial bone cells and in odontoblasts, and showed that the podoplanin deletion in the odontoblasts and osteoblasts does not affect the development and growth of cranial bone and teeth[27]. In the study here, we generated podoplanin-cKO mice in which Cre recombinase driven by the *dmp1* promoter targets the gene of podoplanin exon 3 in cranial bone cells and in odontoblasts. For genotyping of both the tail and cultured calvarial osteoblasts, the gene containing loxP after *Pdpn* exon 3 in the allele of *Pdpn*^{fl} was detected in *Pdpn*$^{fl/fl}$ and *Dmp1-Cre;Pdpn*$^{\Delta/\Delta}$ mice, while the gene without loxP after *Pdpn* exon 3 was detected in wild-type mice (Fig. 3). It is thought that the insertion of the loxP site after *Pdpn* exon 3 was successful. The Cre recombinase gene and the podoplanin gene cleaved by the Cre recombinase were detected in both the tail and cultured calvarial osteoblasts of *Dmp1-Cre;Pdpn*$^{\Delta/\Delta}$ mice, furthermore, the gene flanking *Pdpn* exon 3 was detected in wild-type mice but not detected in *Dmp1-Cre;Pdpn*$^{\Delta/\Delta}$ mice, indicating that the deletion of the loxP-floxed podoplanin gene by *Dmp1*-driven Cre recombinase in *Dmp1-Cre;Pdpn*$^{\Delta/\Delta}$ mice was successful (Fig. 3). The DMP-1 mRNA was detected in both wild-type mice and *Dmp1-Cre;Pdpn*$^{\Delta/\Delta}$ mice while the *Pdpn* mRNA was detected in wild-type mice but not in *Dmp1-Cre;Pdpn*$^{\Delta/\Delta}$ mice, indicating that the deficiency in podoplanin production in *Dmp1*-expressing osteoblasts isolated from *Dmp1-Cre;Pdpn*$^{\Delta/\Delta}$ mice was successful (Fig. 3).

Previously we reported the expression of podoplanin in the teeth[27,31,32]. In the wild-type and *Pdpn*$^{fl/fl}$ mouse tissue, the expression of podoplanin was observed in the odontoblasts, inner and outer enamel epithelial cells and in pre-ameloblasts, and cells in the alveolar bone while it was not observed in the dentin, dental pulp fibroblasts, pre-odontoblasts, periodontal ligament, bone marrow, as we have also reported elsewhere, indicating that the immunostaining is successful. In the *Dmp1-Cre;Pdpn*$^{\Delta/\Delta}$ mouse tissue, the expression of podoplanin was not observed in the odontoblasts, indicating that the conditional knockout of podoplanin in *Dmp1*-expressing cells in *Dmp1-Cre;Pdpn*$^{\Delta/\Delta}$ mice is successful (Fig. 4). There were no abnormalities in the nerve, bone, or tooth development, indicating that the cKO of podoplanin in odontoblasts and osteocytes has no effect on the development and growth of teeth and bone as we have reported elsewhere for *Wnt1-Cre;Pdpn*$^{\Delta/\Delta}$ mice[27]. Therefore, it is thought that podoplanin may not be significantly involved in the mineralization in bone and teeth.

Characteristics of podoplanin-deficient osteoblasts and osteocytes

Our previous study showed that mechanostress induces the production of podoplanin in osteoblasts, and that in cultured osteoblasts the calcification was significantly suppressed by anti-podoplanin and by CLEC-2 protein[29,30]. Considering this, CLEC-2 may be able to cancel the calcification of osteoblast by blocking the maturation of osteoblast via interaction with the CLEC-2 receptor podoplanin in osteocytes under mechanostress. Since the inhibition of podoplanin-mediated calcification requires CLEC-2 in cultured osteoblasts, it may be thought to be natural that podoplanin-cKO mice grew healthily and no abnormalities appeared in bones and teeth[27]. In the study on osteoblasts in three-dimensional culture, the cell process elongation of osteoblasts was suppressed with CLEC-2[30]. There are detailed reports of the cell process elongation via podoplanin and it is thought that podoplanin-cKO may affect the cell process formation of the osteocyte in the bone[21-24]. In the study here, there were no differences in the body growth of *Dmp1-Cre;Pdpn*$^{\Delta/\Delta}$ mice and the wild-type mice, and no differences in calcification and alkaline phosphatase activity in cultured calvarial osteoblasts of the wild-type and *Dmp1-Cre;Pdpn*$^{\Delta/\Delta}$ mice (Fig. 5), in total this suggests that the podoplanin-cKO has no effect on generation of the bone. The cell process elongation was observed in cultured calvarial osteoblasts of wild-type mice while elongation was suppressed in cultured calvarial osteoblasts of *Dmp1-Cre;Pdpn*$^{\Delta/\Delta}$ mice compared with wild-type mice, suggesting that the podoplanin expression may contribute to the formation of osteocyte cell processes. In the electron microscopic study, there were no morphological differences in bone matrix formation and osteocyte distribution in *Dmp1-Cre;Pdpn*$^{\Delta/\Delta}$ mice when compared with wild-type mice (Fig. 6). The highly-developed networks of osteocyte processes were observed in wild-type mouse femurs whereas the process formation was sparser and the network with neighboring cells was more deficient in *Dmp1-Cre;Pdpn*$^{\Delta/\Delta}$ mice than in wild-type mice. In the quantitative analysis, the number and thickness of the cell processes were significantly smaller and thinner in *Dmp1-Cre;Pdpn*$^{\Delta/\Delta}$ mice than in wild-type mice. This could suggest that podoplanin plays a role in the formation of the osteocyte network created by the cell process elongation.

Acknowledgements

This work was supported in part by Grant-in-Aid for Scientific Research (B) 22H03302 (Sawa, Y.) and Grant-in-Aid for Scientific Research (C) 21K10153 (Kanai, T.) from the Japan Society for the Promotion of Science. The funder had no role in study design, data collection and analysis, decision to publish, or preparation of the manuscript.

Conflicts of Interest

The authors indicate no potential conflicts of interest.

References

1. Sawa Y. New trends in the study of podoplanin as a cell morphological regulator. Jpn Dent Sci Rev 46: 165-172, 2010
2. Schacht V, Ramirez MI, Hong YK, Hirakawa S, Feng D, Harvey N, Williams M, Dvorak AM, Dvorak HF, Oliver G and Detmar M. T1a/podoplanin deficiency disrupts normal lymphatic vasculature formation and causes lymphedema. EMBO J 22: 3546-3556, 2003
3. Nose K, Saito H and Kuroki T. Isolation of a gene sequence induced later by tumor-promoting 12-O-tetradecanoylphorbol-13-acetate in mouse osteoblastic cells (MC3T3-E1) and expressed constitutively in ras-transformed cells. Cell Growth Differ 1: 511-518, 1990
4. Farr AG, Berry ML, Kim A, Nelson AJ, Welch MP and Aruffo A. Characterization and cloning of a novel glycoprotein expressed by stromal cells in T-dependent areas of peripheral lymphoid tissues. J Exp Med 176: 1477-1482, 1992
5. Wetterwald A, Hoffstetter W, Cecchini MG, Lanske B, Wagner C, Fleisch H and Atkinson M. Characterization and cloning of the E11 antigen, a marker expressed by rat osteoblasts and osteocytes. Bone 18: 125-132, 1996
6. Hadjiargyrou M, Rightmire EP, Ando T and Lombardo FT. The E11

osteoblastic lineage marker is differentially expressed during fracture healing. Bone 29: 149-154, 2001
7. Schulze E, Witt M, Kasper M, Löwik CW and Funk RH. Immunohistochemical investigations on the differentiation marker protein E11 in rat calvaria, calvaria cell culture and the osteoblastic cell line ROS 17/2.8. Histochem Cell Biol 111: 61-69, 1999
8. Zhang K, Barragan-Adjemian C, Ye L, Kotha S, Dallas M, Lu Y, Zhao S, Harris M, Harris SE, Feng JQ and Bonewald LF. E11/gp38 selective expression in osteocytes: Regulation by mechanical strain and role in dendrite elongation. Mol Cell Biol 26: 4539-4552, 2006
9. Meury T, Akhouayri O, Jafarov T, Mandic V and St-Arnaud R. Nuclear alpha NAC influences bone matrix mineralization and osteoblast maturation *in vivo*. Mol Cell Biol 30: 43-53, 2010
10. Atkins GJ, Rowe PS, Lim HP, Welldon KJ, Ormsby R, Wijenayaka AR, Zelenchuk L, Evdokiou A and Findlay DM. Sclerostin is a locally acting regulator of late-osteoblast/preosteocyte differentiation and regulates mineralization through a MEPE-ASARM-dependent mechanism. J Bone Miner Res 26: 1425-1436, 2011
11. Vazquez M, Evans BA, Riccardi D, Evans SL, Ralphs JR, Dillingham CM and Mason DJ. A new method to investigate how mechanical loading of osteocytes controls osteoblasts. Front Endocrinol 5: 208, 2014
12. Woo SM, Rosser J, Dusevich V, Kalajzic I and Bonewald LF. Cell line IDG-SW3 replicates osteoblast-to-late-osteocyte differentiation *in vitro* and accelerates bone formation *in vivo*. J Bone Miner Res 26: 2634-2646, 2011
13. Chen Z, Wu C, Yuen J, Klein T, Crawford R and Xiao Y. Influence of osteocytes in the *in vitro* and *in vivo* β-tricalcium phosphate-stimulated osteogenesis. J Biomed Mater Res A 102: 2813-2823, 2014
14. Prideaux, M, Loveridge N, Pitsillides AA and Farquharson C. Extracellular matrix mineralization promotes E11/gp38 glycoprotein expression and drives osteocytic differentiation. PLoS One 7: e36786, 2012
15. Zhu D, Mackenzie NC, Millán JL, Farquharson C and MacRae VE. The appearance and modulation of osteocyte marker expression during calcification of vascular smooth muscle cells. PLoS One 6: e19595, 2011
16. Kato Y and Kaneko MK. A cancer-specific monoclonal antibody recognizes the aberrantly glycosylated podoplanin. Sci Rep 4: 5924, 2014
17. Kato Y, Kaneko MK, Kunita A, Ito H, Kameyama A, Ogasawara S, Matsuura N, Hasegawa Y, Suzuki-Inoue K, Inoue O, Ozaki Y and Narimatsu H. Molecular analysis of the pathophysiological binding of the platelet aggregation-inducing factor podoplanin to the C-type lectin-like receptor CLEC-2. Cancer Sci 99: 54-61, 2008
18. Suzuki-Inoue K, Kato Y, Inoue O, Kaneko MK, Mishima K, Yatomi Y, Yamazaki Y, Narimatsu H and Ozaki Y. Involvement of the snake toxin receptor CLEC-2, in podoplanin-mediated platelet activation, by cancer cells. J Biol Chem 282: 25993-26001, 2007
19. Ohizumi I, Harada N, Taniguchi K, Tsutsumi Y, Nakagawa S, Kaiho S and Mayumi T. Association of CD44 with OTS-8 in tumor vascular endothelial cells. Biochim Biophys Acta 1497: 197-203, 2000
20. Martín-Villar E, Megías D, Castel S, Yurrita MM, Vilaró S and Quintanilla M. Podoplanin binds ERM proteins to activate RhoA and promote epithelial-mesenchymal transition. J Cell Sci 119: 4541-4553, 2006
21. Hwang BO, Park SY, Cho ES, Zhang X, Lee SK, Ahn HJ, Chun KS, Chung WY and Song NY. Platelet CLEC2-podoplanin axis as a promising target for oral cancer treatment. Front Immunol 12: 807600, 2021
22. Astarita JL, Cremasco V, Fu J, Darnell MC, Peck JR, Nieves-Bonilla JM, Song K, Kondo Y, Woodruff MC, Gogineni A, Onder L, Ludewig B, Weimer RM, Carroll MC, Mooney DJ, Xia L and Turley SJ. The CLEC-2-podoplanin axis controls the contractility of fibroblastic reticular cells and lymph node microarchitecture. Nat Immunol 16: 75-84, 2015
23. Acton SE, Astarita JL, Malhotra D, Lukacs-Kornek V, Franz B, Hess PR, Jakus Z, Kuligowski M, Fletcher AL, Elpek KG, Bellemare-Pelletier A, Sceats L, Reynoso ED, Gonzalez SF, Graham DB, Chang J, Peters A, Woodruff M, Kim YA, Swat W, Morita T, Kuchroo V, Carroll MC, Kahn ML, Wucherpfennig KW and Turley SJ. Podoplanin-rich stromal networks induce dendritic cell motility via activation of the C-type lectin receptor CLEC-2. Immunity 37: 276-289, 2012
24. Acton SE, Farrugia AJ, Astarita JL, Mourão-Sá D, Jenkins RP, Nye E, Hooper S, van Blijswijk J, Rogers NC, Snelgrove KJ, Rosewell I, Moita LF, Stamp G, Turley SJ, Sahai E and Reis e Sousa C. Dendritic cells control fibroblastic reticular network tension and lymph node expansion. Nature 514: 498-502, 2014
25. Nagai T, Hasegawa T, Yimin, Yamamoto T, Hongo H, Abe M, Yoshida T, Yokoyama A, de Freitas PHL, Li M, Yokoyama A and Amizuka N. Immunocytochemical assessment of cell differentiation of podoplanin-positive osteoblasts into osteocytes in murine bone. Histochem Cell Biol1 55: 369-380, 2021
26. Kajiwara K and Sawa Y. Overexpression of SGLT2 in the kidney of a *P. gingivalis* LPS-induced diabetic nephropathy mouse model. BMC Nephrol 22: 287, 2021
27. Takara K, Maruo N, Oka K, Kaji C, Hatakeyama Y, Sawa N, Kato Y, Yamashita J, Kojima H and Sawa Y. Morphological study of tooth development in podoplanin-deficient mice. PLoS One 12: e0171912, 2017
28. Sawa N, Fujimoto H, Sawa Y and Yamashita J. Alternating differentiation and dedifferentiation between mature osteoblasts and osteocytes. Sci Rep 9: 13842, 2019
29. Takenawa T, Kanai T, Kitamura T, Yoshimura Y, Sawa Y and Iida J. Expression and dynamics of podoplanin in cultured osteoblasts with mechanostress and mineralization stimulus. Acta Histochem Cytochem 51: 41-52, 2018
30. Kanai T, Sawa Y and Sato Y. Cancellation of the calcification in cultured osteoblasts by CLEC-2. J Hard Tissue Biol 30: 53-62, 2021
31. Sawa Y, Iwasawa K and Ishikawa H. Expression of podoplanin in the mouse tooth germ and apical bud cells. Acta Histochem Cytochem 41: 121-126, 2008
32. Imaizumi Y, Amano I, Tsuruga E, Kojima H and Sawa Y. Immunohistochemical examination for the distribution of podoplanin-expressing cells in developing mouse molar tooth germs. Acta Histochem Cytochem 43: 115-121, 2010